The Journal of Chemical Physics

RESEARCH ARTICLE | DECEMBER 12 2025

Performance of GESC and LRESC models for heavy-atom nuclear magnetic shieldings FREE

Andy D. Zapata–Escobar ; Juan I. Melo ; Gustavo A. Aucar

J. Chem. Phys. 163, 224131 (2025)
https://doi.org/10.1063/5.0306490

The Journal of Chemical Physics ARTICLE pubs.aip.org/aip/jcp

Performance of GESC and LRESC models for heavy-atom nuclear magnetic shieldings

Cite as: J. Chem. Phys. 163, 224131 (2025); doi: 10.1063/5.0306490
Submitted: 10 October 2025 • Accepted: 12 November 2025 •
Published Online: 12 December 2025

Andy D. Zapata-Escobar,[1,a] Juan I. Melo,[2,3,b] and Gustavo A. Aucar[1,4,c]

AFFILIATIONS

[1] Institute of Modelling and Innovative Technology, IMIT, Corrientes, Argentina
[2] Universidad de Buenos Aires, Facultad de Ciencias Exactas y Naturales, Departamento de Física, Buenos Aires, Argentina
[3] CONICET - Universidad de Buenos Aires, Instituto de Física de Buenos Aires (IFIBA), Buenos Aires, Argentina
[4] Physics Department, Natural and Exact Science Faculty, Northeastern University of Argentina, Corrientes, Argentina

[a] **Author to whom correspondence should be addressed:** danianescobarv@gmail.com
[b] **Electronic mail:** jmelo@df.uba.ar
[c] **Electronic mail:** gaa@unne.edu.ar

ABSTRACT

Some models have been developed recently to calculate and analyze the electronic origin of the nuclear magnetic shielding tensor. We present here the most recent results of calculations performed with the Geometric Elimination of the Small Component (GESC) model, which represents a partial improvement of the Linear Response Elimination of the Small Component (LRESC) model, particularly concerning diamagnetic contributions. We have found that the accuracy of the diamagnetic contributions obtained with the GESC model is higher than the one obtained with the LRESC model for any molecular system. The difference between the LRESC ($\boldsymbol{\sigma}_d^{LRESC}$) and the four-component ($\boldsymbol{\sigma}^{pp}$) methods is mainly due to the Fermi contact mechanism ($\boldsymbol{\sigma}^{FC,LRESC}$). In the case of the GESC model, the contribution of such electronic mechanism is lowered by a factor of 5/7 with respect to $\boldsymbol{\sigma}^{pp}$. Furthermore, the next important mechanism that contributes to the differences between $\boldsymbol{\sigma}_d^{LRESC}$ and $\boldsymbol{\sigma}^{pp}$ is known as DiaK ($\boldsymbol{\sigma}^{DiaK}$), being its values close to half of that due to $\boldsymbol{\sigma}^{FC,LRESC}$. We analyze here the electronic mechanisms involved in the NMR shielding of halogen atoms of the following family of compounds: HX, IX, and AtX, where X = H, F, Cl, Br, I, At, and the shielding of the central atoms in the following family of molecules: $Sn_{4-i}X_i$ and $PbH_{4-i}X_i$ with i = 1–4 and X = H, F, Cl, Br, I. The calculations were performed at the LRESC-HF/DFT and GESC-HF/DFT levels of theory together with four-component DHF.

I. INTRODUCTION

Several theoretical models developed to describe the response properties of heavy-atom-containing molecules have recently reached a quantitative or semi-quantitative level in reproducing experimental measurements.[1–6] Furthermore, a few of those models have been oriented to the analysis of the involved electronic mechanisms in order to gain new insights into the underlying physics. These methods are based on either two-component (2C) or four-component (4C) frameworks.

Calculations of response properties performed within the 4C framework are usually based on the Dirac–Coulomb–Hartree–Fock (DHF) Hamiltonian,[7,8] and also, the main electronic mechanisms for magnetic properties calculated with polarization propagators can be classified as *ee* (paramagnetic-like) and *pp* (diamagnetic-like).[9,10] The contributions of the *ee*-type mechanisms arise from the contributions of virtual excitations between occupied and unoccupied positive energy molecular orbitals (MOs) in the atomic or molecular spectra. In addition, the contributions of the *pp*-type are obtained after considering the virtual excitations between occupied MOs and unoccupied negative-energy MOs.[10] One of the strengths of this kind of splitting lies in the fact that its nonrelativistic (NR) limit is obtained making the velocity of light (c) go to infinity. In such a case, the *ee* relativistic component of the nuclear magnetic shielding tensor converges to its NR counterpart, the "paramagnetic" component, while the *pp* contribution converges to the "diamagnetic" component.

At present, due to the high cost and complexity of the use of 4C calculations for molecular systems of large size, 2C methodologies are among the most popular. These methods are less computationally expensive, and more importantly, for practical purposes, they

allow the separation of the origin of the whole relativistic effects in several NR electronic mechanisms, which are treated as perturbative corrections, making it easier to get insights into the physics behind them.

One of the most widely used 2C models for calculating NMR spectroscopic parameters is the Zeroth-Order Regular-Approximation (ZORA).[11–14] In a recent study, Vícha *et al.*[15] identified the general electronic structure principles and mechanisms underlying the size and sign of the Spin–Orbit (SO) heavy-atom effect on light atoms (HALA)[16,17] by analyzing the proton NMR chemical shifts of sixth-period hydrides. The same research group has recently published an overview of the periodic trends in HALA effects across heavy-atom-containing diamagnetic compounds throughout the Periodic Table.[3]

There are several other 2C models that have been developed to study linear response molecular properties. One of the earliest is the Douglas–Kroll–Hess (DKH) method,[18–21] which is based on a decoupling of the Dirac Hamiltonian via the Foldy–Wouthuysen transformation.[22,23] The DKH method was first used to describe indirect J-couplings of the Nuclear Magnetic Resonance (NMR) in a series of tetrahedral molecules whose central atom belongs to the carbon group of the Periodic Table. Its results have been found to be in good agreement with 4C methods.[24] In addition, Gauss *et al.*[25–27] developed the model known as Direct Perturbation Theory (DPT). Cheng *et al.*[28] were one of the groups that used DPT to evaluate the size of spin effects compared to spin-free methodologies in thermodynamic molecular energies, dipole moments, and electric field gradients.

On the other hand, the Exact-Two-Component (X2C) model was developed in its simplest way by Jensen in 2005[29] and then applied by Liu *et al.*[30,31] to calculate NMR response properties. In this approach, it is not necessary to calculate an infinite number of terms to accurately reproduce the 4C values of the diamagnetic and paramagnetic components of NMR properties.

Relativistic effects with semi-relativistic Hamiltonians are also treated using the Normalized Elimination of the Small Component (NESC) scheme.[32–34] This method uses the kinetic balance prescription between the small and large components of the 4C spinor basis,[35,36] allowing the construction of a 2C Hamiltonian.

There are two other models that give equivalent electronic mechanisms for including relativistic effects on magnetic response properties, although they are based on different grounds. One of them is based on the no-pair Hamiltonian of a molecular system under the influence of a generic vector potential, first proposed by Fukui *et al.*[37] The model was published by Vaara *et al.* in 2003[38–40] and was based on the Breit–Pauli Perturbation Theory (BPPT) to calculate the magnetic shielding tensor.

The other method was developed in Argentina. An article on its foundation has recently been published.[41] Its starting point considers the full relativistic 4C expression of the second-order Rayleigh–Schrödinger equation. Taking a relativistic Hamiltonian that does not conserve the total number of particles but maintains the total electronic charge constant, the Linear Response Elimination of the Small Component (LRESC) model was first developed in 2003,[42–44] to calculate relativistic effects on the NMR shielding constant.[42,45–50] Due to the clean representation of electronic mechanisms underlying molecular properties, its application has been extended to the treatment of other properties, such as electric field gradients,[50–52] molecular polarizabilities, the molecular rotational g-tensor, and also the likely relationship among different response properties as happens with the NMR shielding and the spin-rotation, and some others.[41] LRESC results for those properties show good agreement with benchmark 4C calculations.

Several versions of the LRESC model were developed. In one of them, Maldonado *et al.*[47] introduced relativistic corrections to the shielding by considering two groups of electronic effects: those corrections that depend or do not depend on the molecular environment of a given nucleus. In this context, they have studied a set of tetrahedral halides with a central atom that belongs to the carbon group of the Periodic Table and showed that one of the weaknesses of the LRESC model could be related to the way it describes the diamagnetic component of the absolute isotropic shielding constant. This is mainly observed for atoms of the sixth row of the Periodic Table, though. In addition, it was also shown that such a component has a large contribution from the inner core electrons.[43,44,53–55]

In 2009, Zaccari *et al.*[45] proposed an alternative expression of the NMR shielding to estimate its diamagnetic component, presenting results for a small group of molecules. This methodology, named Geometric Elimination of the Small Component (GESC), redefines the diamagnetic part of the LRESC model as a geometric sum over positronic states.

One of the goals of the present work is to show a comprehensive study of the formulation by Zaccari *et al.*[45] That formulation was implemented in an in-house version of the DALTON code,[56] within the module of LRESC.[42] Some families of molecular systems were selected to test the results. They include linear molecules, such as H*X*, I*X*, and At*X*, and tetrahedrals $SnH_{4-i}X_i$ and $PbH_{4-i}X_i$, where *X* is a halogen atom and *i* is an integer that runs between 0 and 4. These molecules were selected because some of them have already been studied earlier by the LRESC model. We present here a first systematic study in which the GESC model is shown to improve the estimation of the *pp* component of the shieldings, as compared with the results of the LRESC model.

In Secs. II–V, the theoretical framework, computational details, analysis of results, and conclusions are presented.

II. THEORETICAL FRAMEWORK

In order to show the theoretical grounds of the GESC model in a comprehensive manner, we start by writing the nuclear magnetic shielding tensor using the relativistic polarization propagator theory.[14,57–60] In such a formalism, the shielding tensor ($\boldsymbol{\sigma}_K^{4C}$) is calculated as the linear response of the electronic molecular framework to two external magnetic perturbations: the one produced by the nuclear spin magnetic field *K* (or $\boldsymbol{V}_K$) and the other produced by an external magnetic field $\boldsymbol{B}$ (or $\boldsymbol{V}_B$),

$$\boldsymbol{\sigma}_K^{4C} = \langle\langle \boldsymbol{V}_K; \boldsymbol{V}_B \rangle\rangle = \boldsymbol{b}_K \ \boldsymbol{W}^{-1} \ \boldsymbol{b}_B, \tag{1}$$

being

$$\boldsymbol{V}_K = \boldsymbol{\alpha} \times \frac{\boldsymbol{r}_K}{r_K^3}, \qquad \boldsymbol{V}_B = \frac{\boldsymbol{\alpha} \times \boldsymbol{r}_G}{2}. \tag{2}$$

The elements of the matrix blocks $\boldsymbol{b}_K$ and $\boldsymbol{b}_B$ are known as the perturbators and $\boldsymbol{W}^{-1}$ is known as the principal propagator. Their actual expressions and derivations are given elsewhere.[10]

The shielding of Eq. (1) is written in a basis of molecular orbitals (MOs) as

$$\boldsymbol{\sigma}_K^{4C} = \sum_{ij,ab} \boldsymbol{b}_{K,ia} \left(\boldsymbol{W}^{-1}\right)_{ia,jb} \boldsymbol{b}_{B,jb}, \tag{3}$$

where the indices i and j correspond to occupied MOs and a and b correspond to unoccupied MOs. When the unoccupied MOs belong to the negative-energy branch of the energy spectra, those MOs are written as $\tilde{a}, \tilde{b}$.

Polarization propagators can be calculated at different levels of approach. The first level is known as the Random Phase Approximation (RPA) level,[59] for which

$$\boldsymbol{W} = \begin{pmatrix} \boldsymbol{A} & \boldsymbol{B}^* \\ \boldsymbol{B} & \boldsymbol{A}^* \end{pmatrix}, \tag{4}$$

being

$$\boldsymbol{A}_{ia,jb} = (\varepsilon_i - \varepsilon_a)\delta_{ij}\delta_{ab} + (ai|bj) - (ab|ij), \tag{5}$$

$$\boldsymbol{B}_{ia,jb} = (ja|ib) - (jb|ia). \tag{6}$$

The term $(\varepsilon_i - \varepsilon_a)$ of Eq. (5) corresponds to the difference between one-body energies of occupied MOs and unoccupied positive or negative energy MOs. The other terms on the right-hand side of Eqs. (5) and (6) are the usual two-electron integrals. Thus, Eq. (1) can be written more explicitly as

$$\langle\langle \hat{\boldsymbol{V}}_K; \hat{\boldsymbol{V}}_B \rangle\rangle_E^R = \begin{pmatrix} \tilde{\boldsymbol{V}}_K^{\,ee} & \tilde{\boldsymbol{V}}_K^{\,ep} & \tilde{\boldsymbol{V}}_K^{\,pe} \end{pmatrix} \times \begin{pmatrix} \mathbf{W}^{ee,ee} & \mathbf{W}^{ee,ep} & \mathbf{W}^{ee,pe} \\ \mathbf{W}^{ep,ee} & \mathbf{W}^{ep,ep} & \mathbf{W}^{ep,pe} \\ \mathbf{W}^{pe,ee} & \mathbf{W}^{pe,ep} & \mathbf{W}^{pe,pe} \end{pmatrix}^{-1} \begin{pmatrix} \boldsymbol{V}_B^{\,ee} \\ \boldsymbol{V}_B^{\,ep} \\ \boldsymbol{V}_B^{\,pe} \end{pmatrix}, \tag{7}$$

where each sub-block of the principal propagator matrix and both perturbator matrices are written in such a way that the manifold of basic excitation operators (from which all excited states are derived starting from the ground-state) can be split in two. As is usual, we consider two different types of virtual excitations: the one among occupied MOs and positive-energy unoccupied MOs, denoted as *ee*, and the other that occurs among positive-energy MOs and negative-energy unoccupied MOs, denoted as *ep* and *pe*. As is now well known, the NR paramagnetic-like and diamagnetic-like contributions are obtained by considering both kinds of virtual excitations.[10,57]

It is worth now to sketch how this equation is actually solved.[60] The reduced expression from which the paramagnetic-like and diamagnetic-like components are obtained, without any restrictions on selecting either of the two types of virtual excitations involved, i.e., *ee* and *ep* or *pe*, is as follows:

$$\begin{aligned} \langle\langle \hat{\boldsymbol{V}}_K; \hat{\boldsymbol{V}}_B \rangle\rangle &= \left(\tilde{\boldsymbol{V}}_K^{\,ee}, \tilde{\boldsymbol{V}}_K^{\,ep}, \tilde{\boldsymbol{V}}_K^{\,pe}\right) \begin{pmatrix} \boldsymbol{X}_B^{\,ee} \\ \boldsymbol{X}_B^{\,ep} \\ \boldsymbol{X}_B^{\,pe} \end{pmatrix} \\ &= \boldsymbol{\sigma}^{ee}(K) + \boldsymbol{\sigma}^{ep}(K) + \boldsymbol{\sigma}^{pe}(K) \\ &= \boldsymbol{\sigma}^{ee}(K) + \boldsymbol{\sigma}^{pp}(K), \end{aligned} \tag{8}$$

where the column matrix $\mathbf{X}$ arises from the product between the inverse of the matrix $\mathbf{W}$ and the matrix $\mathbf{V}_B$. Then, there are two well defined and different contributions to $\boldsymbol{\sigma}^{4C}$, which become the usual NR paramagnetic and NR diamagnetic terms when the velocity of light goes to infinity.[9] Therefore, Eq. (8) can be rewritten more explicitly as follows:

$$\begin{aligned} \boldsymbol{\sigma}^{ee}(K) &= \sum_{ij,ab} \langle i|\boldsymbol{V}_K|a\rangle \left(\boldsymbol{W}^{-1}\right)_{ia,jb} \langle b|\boldsymbol{V}_B|j\rangle, \\ \lim_{c\to\infty} \boldsymbol{\sigma}_K^{ee} &= \boldsymbol{\sigma}_p^{NR}(K), \end{aligned} \tag{9}$$

$$\begin{aligned} \boldsymbol{\sigma}^{pp}(K) &= \sum_{ij,\tilde{a}\tilde{b}} \langle i|\boldsymbol{V}_K|\tilde{a}\rangle \left(\boldsymbol{W}^{-1}\right)_{i\tilde{a},j\tilde{b}} \langle \tilde{b}|\boldsymbol{V}_B|j\rangle, \\ \lim_{c\to\infty} \boldsymbol{\sigma}_K^{pp} &= \boldsymbol{\sigma}_d^{NR}(K). \end{aligned} \tag{10}$$

This is the way both components were calculated in this work, using the Dirac code.[61]

All the previous treatment is based on the 4C formalism whose results are usually considered as benchmarks. Their expressions also serve as the starting point for the following 2C formalisms that were initially developed in our research group. In what follows, we provide a brief overview of the LRESC model, in addition to a more extensive overview of the GESC model. More details of these models are provided elsewhere.[41,42,45]

We want to point out first that the second-order correction to the electronic energy is related to the exact polarization propagators by

$$\begin{aligned} E^{(2)}_{\boldsymbol{V}_K,\boldsymbol{V}_B} &= \sum_{n\neq 0} \frac{\langle 0|\boldsymbol{V}|n\rangle\langle n|\boldsymbol{V}|0\rangle}{E_0 - E_n} - \sum_{n\neq vac} \frac{\langle vac|\boldsymbol{V}|n\rangle\langle n|\boldsymbol{V}|vac\rangle}{E_{vac} - E_n} \\ &= \text{Re}\ \langle\langle \boldsymbol{V}_K; \boldsymbol{V}_B \rangle\rangle_{E=0}, \end{aligned} \tag{11}$$

being $\boldsymbol{V} = \boldsymbol{V}_K + \boldsymbol{V}_B$. Equation (11) is one of the most important relations that underlie the developments of the following two theoretical models.

A. The LRESC model

Starting from the 4C matrix elements of the energy expressions of Eq. (11), expanding them as a power series in c^{-1} up to order c^{-4} and introducing some prescriptions, one at the end obtains the 2C LRESC model.[41] The first step consists in dividing the second-order correction to the energy into two terms, which are defined according to their NR limits,[41,42]

$$E^{(2)} = E_a + E_b. \tag{12}$$

Considering only the first term of the right-hand side of Eq. (12), one obtains the paramagnetic-like contribution to $\boldsymbol{\sigma}^{4C}$, and considering the second term, one obtains its diamagnetic-like contribution. This last term arises by taking into account the matrix elements of both the Hamiltonian and the operators V_K and V_B between the N-particle ground state and the manifold of (N + 2)-particle states, which are excited states containing virtual electron–positron pairs in them. Furthermore, given that a magnetic interaction polarizes the vacuum, the second term of Eq. (12) must contain a renormalization term as required within the QED picture.[41,42]

In the LRESC model, most of the terms of both contributions are calculated using expressions that are equivalent to that of Eq. (11),

$$E^{(2)}_{O(\boldsymbol{V}_K)O(\boldsymbol{V}_B)} = \text{Re}\,\langle\langle\, O(\boldsymbol{V}_K); O(\boldsymbol{V}_B)\,\rangle\rangle_{E=0}, \tag{13}$$

where $O(\boldsymbol{V}_K)$ and $O(\boldsymbol{V}_B)$ are here the operators $\boldsymbol{V}_K$ and $\boldsymbol{V}_B$ written in the framework of the LRESC model.

Regarding paramagnetic-like contributions, both LRESC and GESC have the same theoretical expressions. These quantities are

$$\begin{aligned}\boldsymbol{\sigma}_p^{LRESC} = \boldsymbol{\sigma}_p^{GESC} = \boldsymbol{\sigma}_p^{NR} + \boldsymbol{\sigma}^{(Mv+Dw)/p} + \boldsymbol{\sigma}^{SO} \\ + \boldsymbol{\sigma}^{PSOK} + \boldsymbol{\sigma}^{OZK} + \boldsymbol{\sigma}^{SZK} + \boldsymbol{\sigma}^{BSO},\end{aligned} \tag{14}$$

where the corresponding response functions and operators are

$$\boldsymbol{\sigma}^{(Mv+Dw)/p} = \langle\langle H^{OZ}, H^{PSO}, H^{MV} + H^{DW}\rangle\rangle, \tag{15}$$

$$\boldsymbol{\sigma}^{SO} = \langle\langle H^{OZ}, H^{FC+SD}, H^{SO}\rangle\rangle, \tag{16}$$

$$\boldsymbol{\sigma}^{PSOK} = \langle\langle H^{PSOK}, H^{OZ}\rangle\rangle, \tag{17}$$

$$\boldsymbol{\sigma}^{OZK} = \langle\langle H^{PSO}, H^{OZK}\rangle\rangle, \tag{18}$$

$$\boldsymbol{\sigma}^{SZK} = \langle\langle H^{FC+SD}, H^{SZK}\rangle\rangle, \tag{19}$$

$$\boldsymbol{\sigma}^{BSO} = \langle\langle H^{FC+SD}, H^{BSO}\rangle\rangle, \tag{20}$$

where H^{PSO} is the paramagnetic spin–orbit, H^{OZ} is the orbital Zeeman, H^{FC} is the Fermi contact, H^{SD} is the spin dipolar, H^{PSOK} is the kinetic energy correction to the paramagnetic spin–orbit, H^{OZK} is the kinetic energy correction to orbital Zeeman, H^{SZK} is the kinetic energy correction to spin Zeeman, and H^{BSO} is the magnetic external field induced by the spin–orbit coupling. The expressions for the perturbative Hamiltonians can be found in the supplementary material. It is worth mentioning that, right now, both LRESC and GESC models only include the one-body corrections.

In Sec. II B, the LRESC and GESC diamagnetic-like contributions are discussed.

B. The GESC model

In 2009, Zaccari *et al.*[45] proposed the GESC approach to calculate first-order (in terms of $1/c^2$) relativistic corrections though only to the diamagnetic-like contributions of the shielding constant. In this model, the elimination of the small component procedure is applied to the *ep* and *pe* elements of the principal propagator matrix or, equivalently, to the relativistic corrections to the *pp* component of the shieldings.

To start with, one should consider Eq. (12) and, from it, the *pp* term at its lowest order. It is worth to rewrite the second term of the right-hand side of that equation as

$$E_b = \sum_i^{\text{occ}} \sum_{\tilde{a}} \langle i|(\boldsymbol{\alpha}\cdot\boldsymbol{A})|\tilde{a}\rangle \left(\boldsymbol{W}^{-1}\right)_{i\tilde{a},i\tilde{a}} \langle\tilde{a}|(\boldsymbol{\alpha}\cdot\boldsymbol{A})|i\rangle, \tag{21}$$

where, as mentioned above, $|i\rangle$ and $|\tilde{a}\rangle$ stand for the occupied MOs and the negative virtual states, respectively, of the 4C energy spectrum. The operator $(\boldsymbol{\alpha}\cdot\boldsymbol{A})$ is related to the perturbative Hamiltonian that describes the interaction between electrons and appropriate magnetic fields. The matrix $\boldsymbol{\alpha}$ is the Dirac matrix, and the operator $\boldsymbol{A}$ refers to the vector potential that accounts for both the potential due to the nuclear magnetic dipole moment of nucleus K and that of the static external magnetic field. From this perturbative Hamiltonian, one obtains the operators $\mathbf{V}_K$ and $\mathbf{V}_B$ of Eq. (1).

The main novelty of the GESC model consists in the reformulation of the principal propagator matrix as a geometric series, which, in the Pauli spinor basis $(\widetilde{\phi}_i)$, is written as[45]

$$E_b = \frac{1}{2mc^2}\sum_i^{occ} \langle\widetilde{\phi}_i|a\left(1 + \frac{\varepsilon'_e + \boldsymbol{H}^+}{2mc^2}\right)^{-1} a|\widetilde{\phi}_i\rangle, \tag{22}$$

where

$$a = R(\boldsymbol{\sigma}\boldsymbol{A})R - x(\boldsymbol{\sigma}\boldsymbol{A})x, \quad R = 1 - \frac{x^2}{2}, \quad x = \frac{(\boldsymbol{\sigma}\boldsymbol{p})}{2mc}. \tag{23}$$

In Eq. (22), the positive-energy positronic Hamiltonian is

$$H^+ = H_{core} - G, \tag{24}$$

being G the two-body matrix contribution to the Fock matrix.

In order to clarify the discussion of the results, we have used the subscripts d and p to distinguish between paramagnetic-like and diamagnetic-like contribution, respectively.

Then, within the GESC model, the diamagnetic contribution to the shielding tensor $(\boldsymbol{\sigma}_d^{GESC})$ is written as the sum of the following terms:

$$\begin{aligned}\boldsymbol{\sigma}_d^{GESC} = \boldsymbol{\sigma}_d^{NR} + \boldsymbol{\sigma}^{PSO-OZ} + \boldsymbol{\sigma}^{(Mv+Dw)/d} \\ + \boldsymbol{\sigma}^{FC,\ GESC} + \boldsymbol{\sigma}^{R},\end{aligned} \tag{25}$$

while the total diamagnetic contribution within the LRESC model is given by

$$\begin{aligned}\boldsymbol{\sigma}_d^{LRESC} = \boldsymbol{\sigma}_d^{NR} + \boldsymbol{\sigma}^{PSO-OZ} + \boldsymbol{\sigma}^{(Mv+Dw)/d} \\ + \boldsymbol{\sigma}^{FC,\ LRESC} + \boldsymbol{\sigma}^{DiaK},\end{aligned} \tag{26}$$

where

$$\boldsymbol{\sigma}^{PSO-OZ} = -\frac{1}{8m^3c^4}\sum_i^{oc} \langle i|4\left\{\boldsymbol{l}_O, \frac{\boldsymbol{l}_K}{r_K^3}\right\}|i\rangle, \tag{27}$$

$$\boldsymbol{\sigma}^{(Mv+Dw)/d} = \frac{1}{2mc^2}\langle\langle A^2; H^{(Mv+Dw)}\rangle\rangle, \tag{28}$$

$$\begin{aligned}\boldsymbol{\sigma}^{FC,\ GESC} &= \frac{5}{7}\boldsymbol{\sigma}^{FC,\ LRESC} \\ &= \frac{5}{7}\left(\frac{-1}{8m^3c^4}\sum_i^{oc} \langle i|\frac{20\pi\delta(\boldsymbol{r}_K)}{3}|i\rangle\right),\end{aligned} \tag{29}$$

$$\boldsymbol{\sigma}^{DiaK} = \frac{1}{8m^3c^4}\sum_i^{oc} \langle i|\left\{\nabla^2, \frac{\boldsymbol{r}_O^T\boldsymbol{r}_K - \boldsymbol{r}_O\boldsymbol{r}_K^T}{r_K^3}\right\}|i\rangle. \tag{30}$$

In Eqs. (25) and (26), the differences between $\boldsymbol{\sigma}_d^{GESC}$ and $\boldsymbol{\sigma}_d^{LRESC}$ are explicitly shown. The $\boldsymbol{\sigma}^{FC,GESC}$ and $\boldsymbol{\sigma}^{FC,LRESC}$ mechanisms have

different constants [see Eq. (29)]. Furthermore, the terms $\boldsymbol{\sigma}^{DiaK}$ are present only in the LRESC model. The new term in the GESC model, which is analyzed in detail in this work, is

$$\boldsymbol{\sigma}^{R} = \frac{1}{2mc^2}\sum_{i}^{occ}\sum_{\mu\nu\lambda\tau}^{N} C^{*}_{i,\mu}C_{i,\nu}\langle\mu|\frac{\mathbf{r}}{r^3}|\nu\rangle\left[\left(1+\frac{E_e+H_{core}-G}{2mc^2}\right)^{-1}-1\right]_{\mu\nu\lambda\tau} \times C^{*}_{i,\lambda}C_{i,\tau}\langle\lambda|\frac{\mathbf{r}}{2}|\tau\rangle, \quad (31)$$

where the matrix elements $[\ldots]_{\mu\nu\lambda\tau}$ are calculated in the basis of occupied MOs, N is the number of primitive Gaussian functions, c is the velocity of light, and m is the electron mass.

C. Core-dependent and ligand-dependent contributions

We consider here the so-called non-ligand ($\boldsymbol{\sigma}^{nL}$) and ligand ($\boldsymbol{\sigma}^{L}$) terms in which all LRESC terms can be separated, as presented in Refs. 47, 54, and 55. Then, $\boldsymbol{\sigma}^{nL}$ is composed by both paramagnetic-like and diamagnetic-like corrections [see Eqs. (32) and (33)], while $\boldsymbol{\sigma}^{L}$ is composed only by paramagnetic-like corrections [see Eq. (34)].

As paramagnetic-like corrections in the GESC model are the same as those in the LRESC model, we use $\boldsymbol{\sigma}_p^{nL}$ and $\boldsymbol{\sigma}^{L}$ to refer to these methodologies, while the non-ligand corrections for the GESC model are denoted as $\boldsymbol{\sigma}_d^{nL,\ GESC}$.

$\boldsymbol{\sigma}_p^{nL}$ is the addition of $\boldsymbol{\sigma}^{SZK}$ and $\boldsymbol{\sigma}^{BSO}$, while $\boldsymbol{\sigma}^{L}$ is the addition of the following electronic mechanisms: $\boldsymbol{\sigma}^{PSOK}$, $\boldsymbol{\sigma}^{OZK}$, $\boldsymbol{\sigma}^{SO}$, $\boldsymbol{\sigma}^{Mv/p}$, and $\boldsymbol{\sigma}^{Dw/p}$ [see Eq. (34)]. In the case of $\boldsymbol{\sigma}_d^{nL,\ LRESC}$ and $\boldsymbol{\sigma}_d^{nL,\ GESC}$, both include the $\boldsymbol{\sigma}^{PSO-OZ}$, $\boldsymbol{\sigma}^{Mv/d}$, and $\boldsymbol{\sigma}^{Dw/d}$ corrections [see Eqs. (32) and (33)]. The differences between $\boldsymbol{\sigma}_d^{nL,\ LRESC}$ and $\boldsymbol{\sigma}_d^{nL,\ GESC}$ are the same as those that appears between $\boldsymbol{\sigma}_d^{LRESC}$ and $\boldsymbol{\sigma}_d^{GESC}$, as shown in Sec. II B,

$$\boldsymbol{\sigma}^{nL,\ GESC} = \boldsymbol{\sigma}_d^{nL,\ GESC} + \boldsymbol{\sigma}_p^{nL} = \left(\boldsymbol{\sigma}^{R} + \boldsymbol{\sigma}^{FC,\ GESC} + \boldsymbol{\sigma}^{PSO-OZ} + \boldsymbol{\sigma}^{(Mv+Dw)/d}\right) + \left(\boldsymbol{\sigma}^{SZK} + \boldsymbol{\sigma}^{BSO}\right), \quad (32)$$

$$\boldsymbol{\sigma}^{nL,\ LRESC} = \boldsymbol{\sigma}_d^{nL,\ LRESC} + \boldsymbol{\sigma}_p^{nL} = \left(\boldsymbol{\sigma}^{DiaK} + \boldsymbol{\sigma}^{FC,\ LRESC} + \boldsymbol{\sigma}^{PSO-OZ} + \boldsymbol{\sigma}^{(Mv+Dw)/d}\right) + \left(\boldsymbol{\sigma}^{SZK} + \boldsymbol{\sigma}^{BSO}\right). \quad (33)$$

On the other hand, the ligand-type contributions are given by

$$\boldsymbol{\sigma}^{L} \equiv \boldsymbol{\sigma}^{L,\ LRESC} = \boldsymbol{\sigma}^{L,\ GESC} = \boldsymbol{\sigma}^{PSOK} + \boldsymbol{\sigma}^{OZK} + \boldsymbol{\sigma}^{SO} + \boldsymbol{\sigma}^{(Mv+Dw)/p}. \quad (34)$$

III. COMPUTATIONAL DETAILS

To assess the capabilities of GESC, we studied the nuclear magnetic shieldings of one or more than one heavy-atom containing molecule. First, we consider the molecules of set I, which contains H*X*, I*X*, and At*X*, where *X* = H, F, Cl, Br, I, At. On the other hand, the family of molecules of set II contains $Sn_{4-i}X_i$ and $PbH_{4-i}X_i$, with i = 1–4 and *X* = H, F, Cl, Br, I.

Experimental geometries were used for the molecules H*X* and I*X*. They are as follows: 0.9169 Å for HF, 1.2746 Å for HCl, 1.4125 Å for HBr, 1.6090 Å for HI, and 1.9098, 2.3210, 2.4691, and 2.6663 Å for I*X* (*X* = F, Cl, Br, I), respectively.[62] For At-containing molecules, the geometries were optimized at the DHF/dyall.aae4z level of theory. They are as follows: HAt: 1.7117 Å, AtF: 2.0189 Å, AtCl: 2.4765 Å, AtBr: 2.6191 Å, AtI: 2.8224 Å, and At_2: 2.9627 Å. Furthermore, the experimental geometries of SnH_4, $SnCl_4$, and SnC_4H_{12} were taken from the literature.[63–65] The geometries of the other Sn-containing compounds, $SnH_{4-i}X_i$, were taken from theoretical calculations.[46,47] For Pb-containing compounds, $PbH_{4-i}X_i$, their geometries were optimized at the DHF level of theory with the basis set dyall.aae4z[66] for the lead atom and aug-cc-pVTZ-lresc[47] for the rest of the atoms.

To avoid gauge-dependent issues, we set the gauge origin at the site of the studied nucleus in all calculations together with point-like nucleus.

The RPA level of approach was used to perform GESC, LRESC, and 4C calculations. The selected functional was in all cases the BHandHLYP functional.[67] In all calculations, we used dyall.aae4z for set I of molecules, while for set II, we used dyall.aae4z for Sn and Pb and aug-cc-pVTZ-lresc for the rest of the atoms.[46]

All NR calculations were performed using the DALTON code,[56] while 4C calculations were carried out with the DIRAC code.[61]

IV. RESULTS AND DISCUSSION

We show results of relativistic corrections with both models, LRESC and GESC, to isotropic shielding constants, and also, we show trends and importance of paramagnetic and diamagnetic components depending on the molecular environment on selected nuclei. We also performed calculations using these models with one DFT functional, the BHandHLYP functional, which is known to have a better performance for the selected molecules.[68,69] These results are compared with 4C calculations using polarization propagators at the RPA level of approach.[14,57–60]

A. Molecules of set I

In this section, we analyze the electronic mechanisms that are involved in the shieldings of the halogen atoms, *X*, in H*X* molecules. We also show those effects on iodine in I*X* and astatine in At*X* molecules. All GESC and LRESC diamagnetic corrections are included in $\boldsymbol{\sigma}_d^{nL,\ GESC}$ and $\boldsymbol{\sigma}_d^{nL,\ LRESC}$, respectively. These quantities are presented in Table I.

The relativistic corrections calculated with both models increase their values when the atomic number of the atom *X* (Z_X) increases. This means that the main effects involved in the diamagnetic contributions are the well-known heavy atom effects on heavy atom (HAHA), as already discussed in Refs. 46, 70, and 71. It is also observed that for the same atom, the diamagnetic part in both models remains unchanged, with independence of the substituents. In general, the values of the GESC corrections are smaller in absolute value than their LRESC counterparts, and this difference increases with the atomic number of the atom of interest.

As mentioned above, one of the aims of this work is to analyze the behavior of the contribution $\boldsymbol{\sigma}^{R}$, which is calculated with Eq. (31) and implemented in a local version of the DALTON code.[56] It is

TABLE I. Comparison among LRESC and GESC diamagnetic correcting terms for the atoms *X* in H*X*, I in I*X*, and At in At*X* systems, being *X* a halogen atom. All calculations were performed with the dyall.aae4z basis set, and all values are given in ppm.

Atom	$\sigma^{PSO-OZ}+\sigma^{(Mv+Dw)/d}$	$\sigma^{FC,GESC}$ ($\sigma^{FC,LRESC}$)	σ^{R} (σ^{DiaK})	$\sigma_d^{nL,\ GESC}$ ($\sigma_d^{nL,\ LRESC}$)
X				
HF	1.37	−3.32 (−4.64)	−2.49 (−2.04)	−4.44 (−5.30)
HCl	10.56	−23.89 (−33.45)	−18.59 (−15.19)	−31.92 (−38.08)
HBr	102.43	−219.34 (−307.07)	−138.49 (−144.71)	−255.40 (−349.35)
HI	375.82	−777.98 (−1089.17)	−403.61(−524.65)	−805.77 (−1237.99)
HAt	1625.18	−3262.69 (−4567.76)	−1248.44 (−2251.02)	−2885.95 (−5193.60)
I				
IF	375.81	−777.99 (−1089.19)	−403.65 (−524.68)	−805.83 (−1238.07)
ICl	375.75	−777.99 (−1089.19)	−403.72 (−524.76)	−805.96 (−1238.19)
IBr	375.48	−777.99 (−1089.19)	−404.11 (−525.18)	−806.62 (−1238.88)
I_2	374.98	−777.99 (−1089.18)	−404.79 (−525.96)	−807 80 (−1240.16)
IAt	373.37	−777.99 (−1089.18)	−406.75 (−528.43)	−811.37 (−1244.24)
At				
AtF	1625.13	−3262.71 (−4567.79)	−1248.47 (−2251.05)	−2886.05 (−5193.71)
AtCl	1625.08	−3262.70 (−4567.79)	−1248.54 (−2251.12)	−2886.16 (−5193.82)
AtBr	1624.83	−3262.70 (−4567.78)	−1248.91 (−2251.52)	−2886.78 (−5194.47)
AtI	1624.36	−3262.70 (−4567.78)	−1249.55 (−2252.25)	−2887.89 (−5195.67)
At_2	1622.82	−3262.70 (−4567.78)	−1251.43 (−2254.95)	−2891.31 (−5200.06)

easily seen that the behavior of this contribution is consistent with the rest of the diamagnetic corrections. Moreover, the value of σ^R for iodine in HI (−403.61 ppm) is close to the result published in Ref. 45 (−385.20 ppm). The difference is due to the different basis set used in both calculations.

In Table II and Fig. 1, we show the isotropic values of paramagnetic, σ_p, and diamagnetic, σ_d, shielding components calculated using both the LRESC and GESC models. These results are shown for the atom *X* in the H*X* molecules and for iodine and astatine in I*X* and At*X* molecules, respectively. We also provide the *ee* and *pp* contributions to the 4C shielding for the same atoms, denoted as σ^{ee} and σ^{pp}, respectively.

The values of the total shielding constants, σ^{LRESC}, σ^{GESC}, and σ^{4C}, increase with the atomic number of the studied nucleus. There is the special case of iodine in IAt, where the paramagnetic term is not very well reproduced (see Table II and Fig. 1). This system suffers from a quasi-instability in the estimation of σ^{ee} in 4C calculations. In contrast, σ_p is closer to σ^{ee} for astatine in At*X* and for iodine in I*X* when the electronic correlation is considered at the DFT level of theory with the functional BHandHLYP.[67] Moreover, DFT calculations are mandatory to overcome quasi-instabilities in AtI. We choose BHandHLYP[67] to include electronic correlation because Melo *et al.*[69] had shown that this functional improves the accuracy of the LRESC model with respect to the σ^{4C} values. Furthermore, Hanni *et al.*[68] reported that working with this functional, the experimental temperature dependence of the second virial coefficient of the ^{129}Xe shielding is also reproduced.[74]

The diamagnetic components calculated with the GESC model are closer to their relativistic counterparts as compared to those obtained with the LRESC model. The improvement in the GESC description becomes more pronounced as the atoms in the molecular system become heavier, as shown in Table II and Fig. 1. When the atom of interest belongs to the p-block of the Periodic Table, the estimation error for σ_d^{GESC} is one-third of the error of σ_d^{LRESC}. Among all corrections involved in the diamagnetic part of LRESC, Eq. (33), $\sigma^{FC,LRESC}$ represents the main electronic mechanism responsible for making that σ_d^{LRESC} goes away from σ^{pp} (see Table I). The second correction responsible for the difference between σ_d^{LRESC} and σ^{pp} is σ^{DiaK}, which represents half of $\sigma^{FC,LRESC}$. In this sense, with the change in the corresponding constant of $\sigma^{FC,GESC}$ and its new term, σ^R, the GESC model becomes a more suitable methodology, than LRESC, for the description of the relativistic effect associated with σ^{pp}.

The paramagnetic component of the isotropic shielding constant, σ_p, which is the same for both LRESC and GESC models, reproduces fairly well σ^{ee} for atoms up to the fifth row of the Periodic Table. For astatine, this behavior is maintained only when astatine is attached to lighter atoms than itself or is bonded to less electronegative atoms than fluorine. However, σ^{GESC} and σ^{LRESC} diverge from σ^{4C} for iodine in I*X* when the atom *X* is either fluorine or astatine. Then, the lack of quantitative reproducibility of LRESC (and GESC) compared to 4C values is primarily due to their paramagnetic component.

Regarding the behavior of the shielding of the *X* atom in H*X*, iodine in I*X*, and astatine in At*X*, it is useful to consider the ligand-type, σ^L, and non-ligand-type, σ_p^{nL}, description of σ_p. The values of these quantities are shown in Table III at the HF and DFT levels of theory. The electronic correlation is negligible for σ_p^{nL}. Instead, the

TABLE II. Isotropic shielding constants for halogen *X* atoms in H*X*, iodine in I*X*, and astatine in At*X* molecules, at the LRESC, GESC, and DHF levels of theory. DFT/BHandHLYP calculations are given in parentheses, and the dyall.aae4z basis set was used in all calculations, which are given in ppm.

	Paramagnetic and ee		Diamagnetic and pp			Total			
	$\sigma_p^{LRESC} \equiv \sigma_p^{GESC} \equiv \sigma_p$	σ^{ee}	σ_d^{LRESC}	σ_d^{GESC}	σ^{pp}	σ^{LRESC}	σ^{GESC}	σ^{4C}	References
X									
HF	−58.36 (−59.61)	−59.17 (−60.44)	476.70 (476.97)	477.58 (477.82)	476.92 (477.14)	418.34 (417.36)	419.21 (418.21)	417.75 (416.69)	419.3,[a] 418.4,[b] 410 ± 6[c]
HCl	−132.54 (−140.26)	−139.80 (−147.65)	1112.42 (1112.80)	1118.59 (1118.90)	1121.65 (1122.05)	979.89 (972.54)	986.05 (978.64)	981.85 (974.40)	988.8,[a] 984.5[b]
HBr	124.56 (84.73)	37.29 (−3.66)	2778.88 (2779.07)	2872.83 (2872.82)	2914.11 (2914.47)	2903.44 (2863.80)	2997.39 (2957.56)	2951.40 (2910.81)	3013.5,[a] 2959.4[b]
HI	1285.81 (1195.80)	1001.73 (891.88)	4269.77 (4270.11)	4702.0 (4702.00)	4884.45 (4885.42)	5555.58 (5465.91)	5987.81 (5897.80)	5886.18 (5777.29)	5563.6,[a] 5913.7[b]
HAt	7853.57 (7590.23)	10 226.50 (9320.52)	5372.13 (5372.10)	7679.78 (7679.32)	8594.57 (8597.25)	13 225.70 (12 962.34)	15 533.35 (15 269.55)	18 821.07 (17 917.77)	19 592.7[b]
I									
IF	−3169.80 (−4518.15)	−3993.91 (−5026.47)	4307.15 (4307.56)	4739.39 (4739.46)	4923.76 (4923.97)	1137.35 (−210.59)	1569.58 (221.31)	929.86 (−102.50)	
ICl	−541.63 (−1280.46)	−1200.27 (−1845.83)	4331.87 (4332.25)	4764.11 (4764.15)	4947.49 (4948.07)	3790.24 (3051.79)	4222.47 (3483.69)	3747.22 (3102.24)	
IBr	−605.51 (−655.86)	37.44 (−1213.18)	4395.66 (4396.03)	4827.92 (4827.96)	5011.09 (5011.63)	4433.10 (3740.17)	4865.36 (4172.10)	4405.57 (3798.45)	
I_2	789.29 (441.11)	456.81 (105.68)	4448.13 (4448.49)	4880.50 (4880.52)	5063.24 (5063.85)	5237.42 (4889.60)	5669.78 (5321.62)	5520.05 (5169.53)	5303.4[a]
IAt	−916.06 (−592.60)	1263.87[d] (428.12)	4540.32 (4540.67)	4973.19 (4973.20)	5160.99 (5156.09)	3624.26 (3948.06)	4057.12 (4380.60)	6424.86 (5584.21)	
At									
AtF	6672.39 (369.42)	7700.79 (1266.36)	5407.53 (5407.49)	7715.19 (7714.69)	8635.97 (8636.52)	12 079.91 (5776.91)	14 387.58 (8084.11)	16 336.76 (9902.89)	
AtCl	8422.69 (4648.30)	7000.88 (3764.23)	5430.22 (5430.16)	7737.88 (7737.36)	8656.59 (8658.05)	13 852.91 (10 078.46)	16 160.58 (12 385.66)	15 657.47 (12 422.28)	
AtBr	9196.79 (5696.74)	4850.65 (4265.51)	5490.73 (5490.67)	7798.42 (7797.90)	8716.34 (8718.28)	14 687.52 (11 187.41)	16 995.21 (13 494.64)	13 566.99 (12 983.79)	
AtI	9276.16 (7743.20)	187 649.66[d] (5763.42)	5540.57 (5540.07)	7848.35 (7847.81)	8774.60 (8767.23)	14 816.73 (13 283.27)	17 124.51 (15 590.59)	196 424.25 (14 530.66)	
At_2	6344.73 (5394.36)	8714.18 (7341.38)	5629.38 (5629.77)	7938.13 (7846.24)	8853.68 (8856.30)	11 974.11 (11 024.12)	14 282.85 (13 240.60)	17 567.85 (16 197.68)	

[a]Results of 2C NESC-GIAO calculations with Gaussian nucleus, taken from Ref. 72.
[b]Results of 4C calculations with Gaussian nucleus, taken from Refs. 39 and 40.
[c]Experimental results taken from Ref. 73.
[d]The calculation presents quasi-instability.

influence of the electronic correlation on σ^L increases drastically as a function of the atomic number of the atom of interest or its substituents. We did not make an exhaustive analysis of this within the LRESC framework of the non-ligand- and ligand-type contributions because it is not the goal of this work to do it. In addition, some other works with this kind of studies were published by authors of our group.[47,54,55,75]

B. Molecules of set II

As mentioned, the second set of molecules chosen to test the GESC model consists of the family of $SnH_{4-i}X_i$ and $PbH_{4-i}X_i$ molecules, where i = 0–4 and X = F, Cl, Br, I. Table VI and Fig. 2 present LRESC, GESC, and 4C results divided into paramagnetic and diamagnetic terms. Moreover, it is well known that the shielding of Sn and Pb in the studied systems does not suffer from quasi-instabilities.[46,47] Therefore, the electronic correlation is not necessary to be considered in this section.

For Sn, the diamagnetic GESC values, σ_d^{GESC}, are closer to the 4C calculations, σ^{pp}, than LRESC values, σ_d^{LRESC}. The difference between σ_d^{LRESC} and σ^{pp} in the whole set of $SnH_{4-i}X_i$ structures is around 499 ppm. In contrast, the estimation error of σ_d^{GESC} is once again one-third of σ_d^{LRESC}. Moreover, the paramagnetic part, σ_p, gets closer to σ^{ee} as the number of F or I substituents around Sn increases. Then, σ^{GESC}(Sn) becomes closer to σ^{4C}(Sn) as the atomic number of substituents increases.

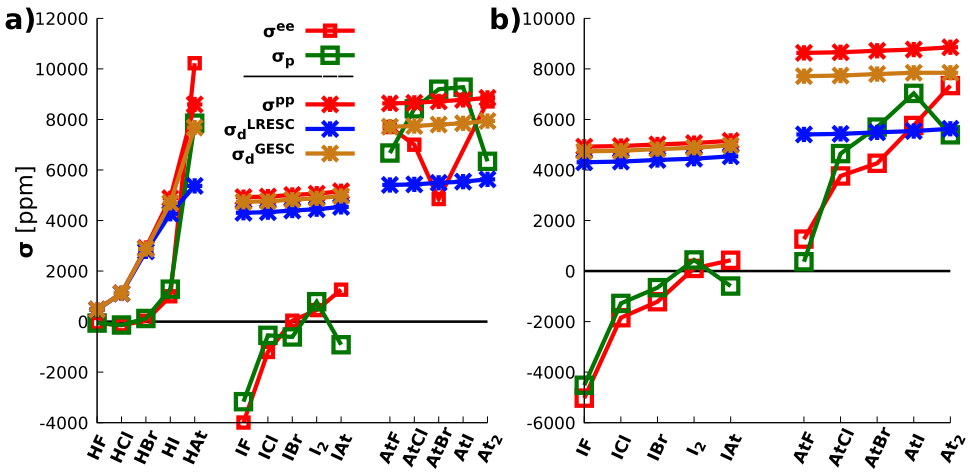

FIG. 1. Isotropic values of σ^{ee} and σ^{pp}, together with σ_p, σ_d^{LRESC}, and σ_d^{GESC} for atoms X in HX, iodine in IX, and astatine in AtX. All calculations were performed with the dyall.aae4z basis set, and the results are given in ppm. In panel (a), HF and DHF results are given, and in panel (b), correlated results are shown with the functional BHandHLYP.

TABLE III. Isotropic values of σ^L and σ_p^{nL} correction for X in HX and iodine and astatine in IX and AtX molecules, respectively, being X a halogen atom. Calculations were performed at the RPA and Hartree–Fock and BHandHLYP levels of theory with the basis set dyall.aae4z. All results are given in ppm.

	HF		BHandHLYP	
	σ^L	σ_p^{nL}	σ^L	σ_p^{nL}
HF	0.43	9.25	0.47	9.24
HCl	3.36	64.06	3.19	64.11
HBr	41.11	578.76	37.57	579.02
HI	170.88	2087.00	149.15	2087.64
HAt	854.24	8781.13	725.60	8782.60
IF	1730.40	2089.78	1048.38	2089.13
ICl	1014.81	2088.58	704.45	2088.68
IBr	780.13	2088.29	506.64	2088.57
I_2	91.23	2087.94	49.21	2088.41
IAt	−1922.39	2087.37	−1286.36	2088.32
AtF	10 492.10	8790.37	5497.22	8786.80
AtCl	7316.48	8786.85	4510.09	8785.96
AtBr	6509.44	8785.76	3926.85	8785.57
AtI	3999.43	8784.37	2465.83	8785.02
At_2	325.57	8783.15	75.92	8784.77

Regarding the total diamagnetic contribution to the shielding of lead, the GESC model is shown to be more suitable for the description of the relativistic effect associated with σ^{pp}. This produces that σ^{GESC} for lead is closer to σ^{4c}(Pb). It is worth mentioning that the differences between the GESC and LRESC values and the 4C value for lead increase as the number of heavy atoms around it increases.

The values of σ^L and σ_p^{nL} for set II of molecules are shown in Table IV. The values of σ^L tend to be more positive with the number of heavy atoms around the center atom for Sn and Pb. The behavior of σ^L for tin is such that σ_p is closer to σ^{ee}, while for lead, it is not enough. Then, the differences of the contributions of LRESC and GESC with respect σ^{4C} are, in general, due to ligand-type corrections in atoms belonging to the sixth-row of the Periodic Table.

Another important observation is that the differences of the shieldings of both models, GESC and LRESC, decrease as the molecular system increases its symmetry. This is particularly clear as σ_d^{GESC} and σ_d^{LRESC} become closer to σ^{pp} when comparing $SnH_{4-i}X_i$ with IX. It is important to stress that the GESC and LRESC models become less efficient in reproducing quantitatively the values of $\sigma^{pp}(Sn)$ as the atomic number of the substituent increases in SnH4 – iX$_i$. In addition, for the family of $PbH_{4-i}X_i$ compounds, the deviation of the value of shieldings modeled by GESC and LRESC relative to the total 4C values increases due to the fact that the effect of the environment is less well reproduced when the numbers of Br and I atoms increase. This is specially observed in the difference between σ_p(Pb) and σ^{ee}(Pb).

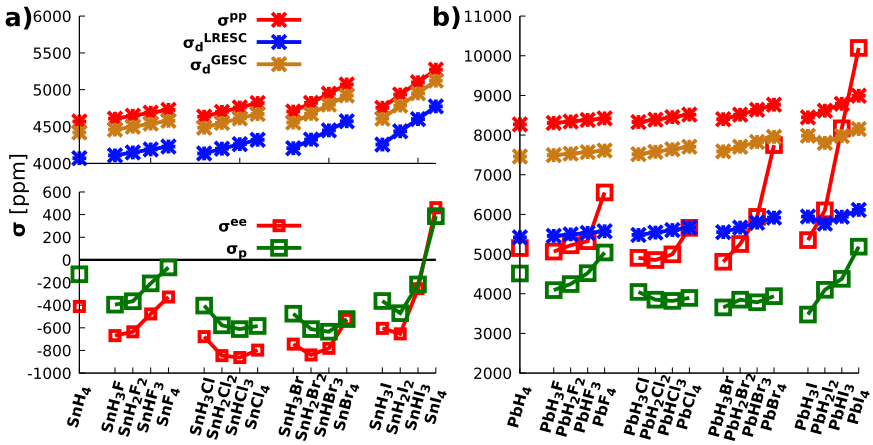

FIG. 2. Isotropic values of σ^{ee} and σ^{pp}, together with σ_p, σ_d^{LRESC}, and σ_d^{GESC}. (a) Sn atoms in $SnH_{4-i}X_i$ and (b) Pb in $PbH_{4-i}X_i$, where X is a halogen atom and i = 0–4. All values are in ppm.

TABLE IV. Isotropic values of σ^L and σ_p^{nL} for Sn and Pb for set II of molecules. Calculations were performed at the HF level of theory with the dyall.aae4z basis set for the central atoms and the aug-cc-pVTZ-lresc basis set for the substituents. All values are given in ppm.

	σ^L	σ_p^{nL}		σ^L	σ_p^{nL}
SnH_4	−35.91	1744.84	PbH_4	−143.20	7866.88
SnH_3F	−34.88	1744.87	PbH_3F	−137.66	7866.94
SnH_2F_2	−26.14	1744.85	PbH_2F_2	−108.11	7866.85
$SnHF_3$	−14.62	1744.67	$PbHF_3$	−170.75	7866.44
SnF_4	−3.02	1744.34	PbF_4	40.43	7866.19
SnH_3Cl	−32.32	1744.89	PbH_3Cl	−151.73	7866.94
SnH_2Cl_2	−25.12	1744.97	PbH_2Cl_2	−153.28	7867.06
$SnHCl_3$	0.51	1744.97	$PbHCl_3$	1.07	7714.84
$SnCl_4$	50.34	1744.83	$PbCl_4$	−65.32	7866.40
SnH_3Br	−14.88	1745.13	PbH_3Br	−439.65	7867.33
SnH_2Br_2	63.64	1745.42	PbH_2Br_2	−23.26	7867.52
$SnHBr_3$	220.35	1745.82	$PbHBr_3$	137.44	7867.89
$SnBr_4$	483.20	1746.42	$PbBr_4$	439.19	7868.39
SnH_3I	52.50	1745.20	PbH_3I	−17.77	7867.26
SnH_2I_2	218.17	1745.61	PbH_2I_2	261.26	7867.93
$SnHI_3$	738.89	1746.52	$PbHI_3$	881.69	7868.84
SnI_4	1584.53	1747.65	PbI_4	1969.15	7870.05

TABLE V. Chemical shifts for tin in $SnCl_4$, $SnBr_4$, and SnI_4 with respect to SnH_4, were calculated with relativistic, δ^{4C}, LRESC, δ^{LRESC}, GESC, δ^{GESC}, and nonrelativistic, δ^{NR}, methods as experimental values; δ^{exp} uses SnH_4 as the reference. LRESC and GESC calculations are performed at the HF level of theory, while 4C calculations are performed at the DHF level of theory. DFT/BHandHLYP calculations are given in parentheses.

	δ^{NR} (Sn)	δ^{LRESC} (Sn)	δ^{GESC} (Sn)	δ^{4C} (Sn)	δ^{exp} (Sn)
SnH_4	0.0	0.0	0.0	0.0	0.0[a]
$SnCl_4$	293.2 (415.9)	207.5 (327.3)	207.5 (327.3)	135.3 (258.1)	350.0[b]
$SnBr_4$	412.3 (560.1)	−105.0 (−123.9)	−105.1 (−124.0)	−387.0 (−433.6)	−138.0[b]
SnI_4	399.2 (562.0)	−1215.7 (−1621.0)	−1216.2 (−1621.5)	−1577.1 (−1793.6)	−1201.0[b]

[a] δ^{exp}(Sn) = 500 ppm, taken from Ref. 76.
[b] Taken from Ref. 77.

TABLE VI. Isotropic shielding constants calculated with LRESC, GESC, and 4C models divided into paramagnetic and diamagnetic terms for comparison. Calculations are performed on Sn in $SnH_{4-i}X_i$ and Pb in $PbH_{4-i}X_i$, X = F, Cl, Br, I and i = 1–4. The basis set used is dyall.aae4z for central atoms, while the aug-cc-pVTZ-lresc basis set is used for substituents. All values are given in ppm.

	Paramagnetic and ee		Diamagnetic and pp			Total				Paramagnetic and ee		Diamagnetic and pp			Total		
Sn	$\sigma_p^{LRESC} \equiv \sigma_p^{GESC} \equiv \sigma_p$	σ^{ee}	σ_d^{LRESC}	σ_d^{GESC}	σ^{pp}	σ^{LRESC}	σ^{GESC}	σ^{4C}	Pb	$\sigma_p^{LRESC} \equiv \sigma_p^{GESC} \equiv \sigma_p$	σ^{ee}	σ_d^{LRESC}	σ_d^{GESC}	σ^{pp}	σ^{LRESC}	σ^{GESC}	σ^{4c}
SnH_4	−126.66	−411.97	4070.74	4420.51	4569.27	3944.08	4293.85	4157.30	PbH_4	4510.27	5151.92	5422.62	7459.04	8269.61	9933.17	11 969.31	13 421.53
SnH_3F	−395.70	−669.22	4109.18	4458.95	4607.77	3713.48	4063.25	3938.54	PbH_3F	4091.93	5063.77	5459.08	7495.21	8306.06	9551.01	11 587.13	13 369.83
SnH_2F_2	−365.29	−635.34	4148.29	4498.06	4646.87	3783.00	4132.77	4011.52	PbH_2F_2	4243.79	5221.46	5495.66	7531.75	8343.25	9739.45	11 775.54	13 564.71
$SnHF_3$	−207.51	−477.65	4189.53	4539.29	4688.04	3982.02	4331.78	4210.39	$PbHF_3$	4518.01	5326.01	5533.75	7569.82	8380.52	10 051.76	12 087.83	13 706.53
SnF_4	−66.50	−328.15	4229.03	4578.78	4727.47	4162.53	4512.27	4399.32	PbF_4	5039.55	6554.49	5574.14	7610.20	8420.74	10 613.69	12 649.75	14 975.23
SnH_3Cl	−403.42	−677.83	4135.33	4485.10	4633.92	3731.91	4081.69	3956.09	PbH_3Cl	4044.92	4904.0	5481.77	7517.90	8328.71	9526.70	11 562.82	13 232.72
SnH_2Cl_2	−578.52	−845.96	4199.97	4549.75	4698.60	3621.45	3971.22	3852.65	PbH_2Cl_2	3850.88	4850.55	5542.39	7578.51	8389.45	9393.27	11 429.39	13 240.0
$SnHCl_3$	−611.33	−862.30	4260.62	4610.39	4759.27	3649.29	3999.06	3896.97	$PbHCl_3$	3818.78	4993.98	5604.86	7640.97	8451.97	9423.64	11 459.75	13 445.95
$SnCl_4$	−584.01	−797.24	4320.57	4670.34	4819.24	3736.56	4086.33	4022.0	$PbCl_4$	3895.59	5661.70	5669.31	7705.41	8516.10	9564.89	11 601.00	14 177.80
SnH_3Br	−475.52	−743.93	4205.41	4555.22	4704.03	3729.89	4079.70	3960.10	PbH_3Br	3654.62	4806.28	5553.86	7590.03	8400.76	9208.48	11 244.64	13 207.05
SnH_2Br_2	−611.40	−839.55	4323.09	4672.92	4821.83	3711.69	4061.52	3982.28	PbH_2Br_2	3849.78	5253.62	5668.03	7704.21	8515.19	9517.80	11 553.99	13 768.81
$SnHBr_3$	−634.48	−781.17	4447.77	4797.63	4946.61	3813.28	4163.15	4165.44	$PbHBr_3$	3784.63	5937.73	5791.00	7827.21	8638.30	9575.63	11 611.84	14 576.03
$SnBr_4$	−522.79	−526.59	4571.89	4921.78	5070.84	4049.10	4398.99	4544.25	$PbBr_4$	3939.45	7747.63	5918.13	7954.36	8765.53	9857.58	11 893.81	16 513.16
SnH_3I	−362.80	−604.83	4256.19	4606.10	4755.02	3893.39	4243.30	4150.19	PbH_3I	3474.59	5352.70	5945.52	7981.78	8446.08	9420.11	11 456.37	13 798.78
SnH_2I_2	−470.70	−653.20	4435.35	4785.40	4934.48	3964.66	4314.70	4281.27	PbH_2I_2	4100.11	6103.03	5767.10	7803.48	8614.69	9867.20	11 903.59	14 717.72
$SnHI_3$	−216.96	−254.70	4601.60	4951.77	5101.07	4384.65	4734.81	4846.37	$PbHI_3$	4375.60	8170.30	5941.49	7978.01	8789.53	10 317.10	12 353.62	16 959.83
SnI_4	386.43	461.21	4773.31	5123.60	5273.14	5159.73	5510.02	5734.36	PbI_4	5187.14	10 196.30	6113.95	8150.58	8991.48	11 301.09	13 337.72	19 187.77

Finally, since there are experimental values available,[76,77] we show the chemical shifts of tin in $SnCl_4$, $SnBr_4$, and SnI_4 considering the SnH_4 molecule as the reference. Experimental, δ^{exp}, relativistic, δ^{4C}, LRESC, δ^{LRESC}, GESC, δ^{GESC}, and non-relativistic, δ^{NR}, chemical shifts are presented in Table V.

Results of δ^{LRESC} and δ^{GESC} for tin are both close to the value of δ^{exp}. In contrast, the results of δ^{4C} deviates from δ^{exp} because $\boldsymbol{\sigma}^{ee}$ is underestimated, as is shown in Table VI. The electronic correlation makes that δ^{LRESC} and δ^{GESC} become closer to δ^{exp}. The exception appears for SnI_4, where quasi-relativistic and relativistic calculations with DFT move away from δ^{exp}. The improvement in electronic correlation for tin in $SnCl_4$ is primarily due to δ^{NR}, as the gap between results with or without DFT calculations is comparable to those obtained with δ^{LRESC} and δ^{GESC}.

The relativistic corrections are the ones mainly responsible for getting semi-quantitative accuracy in the estimation of the experimental value for tin in the $SnBr_4$ molecule with the LRESC and GESC models. This is because the values of δ^{LRESC} and δ^{GESC} do not differ much among themselves although δ^{NR} increases in magnitude when electronic correlation is included. In the case of SnI_4, the results of quasi-relativistic and relativistic methodologies with electronic correlation overestimate the experimental values, possibly because the functional BHandHLYP[67] is not suitable for modeling the chemical shift in this system due to its parameterization, or because dynamic electronic correlation starts to play a more significant role.

V. CONCLUSIONS

We have given a thorough analysis of the GESC methodology applied on two selected sets of molecules, which contain one or several heavy atoms. We may state that the results with the GESC model improve the estimation of the values of $\boldsymbol{\sigma}^{pp}$ with respect to those of the LRESC model. For the development of this work, a new and more efficient implementation of the GESC model was written in an in-house version of the Dalton[56] program within the LRESC module.[42]

The results given by $\boldsymbol{\sigma}^{R}$ correction for sets I and II of molecules reproduce the trends observed in other diamagnetic corrections for nuclear magnetic shieldings. In addition, the $\boldsymbol{\sigma}^{R}$ value for iodine in HI resembles the values reported by Zaccari *et al.* in Ref. 45.

The contribution $\boldsymbol{\sigma}_d^{nL,LRESC}$ overestimates the relativistic correction, causing that $\boldsymbol{\sigma}_d^{LRESC}$ goes away from $\boldsymbol{\sigma}^{pp}$, while $\boldsymbol{\sigma}_d^{GESC}$ is, in fact, closer to it. The overestimation obtained with the LRESC model can be attributed to two electronic mechanisms: (i) the $\boldsymbol{\sigma}^{FC,LRESC}$ correction, which is 7/5 times larger than its counterpart in the GESC model, and (ii) the $\boldsymbol{\sigma}^{DiaK}$ correction, which is half the value of $\boldsymbol{\sigma}^{FC,LRESC}$.

The values of $\boldsymbol{\sigma}_d^{GESC}$ show a more significant improvement with heavier atoms. For example, in H*X* molecules, the improvement is more pronounced when *X* is Br, I, or At, whereas in other systems, it is independent of the substituents.

Electronic correlation is necessary to eliminate quasi-instabilities and restore the trend of the paramagnetic-like correction for astatine in At*X* molecules. Moreover, the effect of electronic correlation on the non-ligand-type corrections in GESC and LRESC is less pronounced than that on the ligand-type corrections. Another important feature is that the deviations of $\boldsymbol{\sigma}_d^{GESC}$ and $\boldsymbol{\sigma}_d^{LRESC}$ from $\boldsymbol{\sigma}^{pp}$ are smaller in $SnH_{4-i}X_i$ than in IX, although the deviations of the GESC and LRESC results from 4C values increase with the number of Br and I atoms in $SnH_{4-i}X_i$.

However, the differences with the estimation of $\boldsymbol{\sigma}^{4C}$ in both LRESC and GESC models are primarily due to the paramagnetic component. Therefore, in order to obtain more quantitative results for the heaviest-atom containing molecules, it would be necessary to develop a new methodology regarding higher-order corrections for the paramagnetic components.

SUPPLEMENTARY MATERIAL

In the supplementary material, we present (i) the explicit expression of the perturbative Hamiltonian in the LRESC model and (ii) the values of the different corrections to the diamagnetic component in the LRESC and GESC models for the atom *Y* in the $YH_{4-i}X$ systems, where *Y* is Sn and Pb atoms, *X* is a halogen atom, and $i = 0$–4.

ACKNOWLEDGMENTS

We would also like to acknowledge the Institute of Modelling and Innovative Technology, IMIT, of the National Scientific and Technical Research Council (CONICET) and the Northeastern University of Argentina (UNNE) for the support and for providing access to the IMIT high-performance computing cluster.

AUTHOR DECLARATIONS

Conflict of Interest

The authors have no conflicts to disclose.

Author Contributions

Andy D. Zapata–Escobar: Conceptualization (equal); Data curation (equal); Formal analysis (equal); Investigation (equal); Methodology (equal); Project administration (equal); Software (equal); Supervision (equal); Validation (equal); Visualization (equal); Writing – original draft (equal); Writing – review & editing (equal). **Juan I. Melo**: Conceptualization (equal); Data curation (equal); Formal analysis (equal); Investigation (equal); Methodology (equal); Project administration (equal); Resources (equal); Software (equal); Supervision (equal); Validation (equal); Visualization (equal); Writing – original draft (equal); Writing – review & editing (equal). **Gustavo A. Aucar**: Conceptualization (equal); Data curation (supporting); Formal analysis (supporting); Funding acquisition (lead); Investigation (equal); Methodology (equal); Project administration (lead); Resources (lead); Supervision (equal); Validation (equal); Visualization (supporting); Writing – original draft (equal); Writing – review & editing (equal).

DATA AVAILABILITY

The data that support the findings of this study are available within the article and its supplementary material and also from the corresponding author upon reasonable request.

REFERENCES

[1] I. L. Rusakova and L. B. Krivdin, "An introduction to quantum chemical methods for the calculation of NMR parameters: Different sides of the coin," in *NMR Spectroscopic Parameters. Theories and Models, Computational Codes and Calculations*, edited by G. A. Aucar (Royal Society of Chemistry, 2025), Chap. 1, pp. 3–61.

[2] I. L. Rusakova and Y. Y. Rusakov, "Relativistic effects from heavy main group p–elements on the NMR chemical shifts of light atoms: From pioneering studies to recent advances," Magnetochemistry **9**, 24 (2023).

[3] J. Vicha, J. Novotný, S. Komorovsky, M. Straka, M. Kaupp, and R. Marek, "Relativistic heavy–neighbor–atom effects on NMR shifts: Concepts and trends across the periodic table," Chem. Rev. **120**, 7065–7103 (2020).

[4] Y. J. Franzke and F. Weigend, "NMR shielding tensors and chemical shifts in scalar-relativistic local exact two-component theory," J. Chem. Theory Comput. **15**, 1028–1043 (2019).

[5] S. Moncho and J. Autschbach, "Relativistic zeroth-order regular approximation combined with nonhybrid and hybrid density functional theory: Performance for NMR indirect nuclear spin–spin coupling in heavy metal compounds," J. Chem. Theory Comput. **6**, 223–234 (2010).

[6] M. Kaupp, M. Buhl, and V. G. Malkin, *Calculation of NMR and EPR Parameters* (Wiley Online Library, 2004).

[7] K. G. Dyall and K. Fægri, Jr., *Introduction to Relativistic Quantum Chemistry* (Oxford University Press, 2007).

[8] M. Reiher and A. Wolf, *Relativistic Quantum Chemistry* (Wiley-VCH, 2009).

[9] G. A. Aucar, T. Saue, L. Visscher, and H. J. A. Jensen, "On the origin and contribution of the diamagnetic term in four–component relativistic calculations of magnetic properties," J. Chem. Phys. **110**, 6208–6218 (1999).

[10] G. A. Aucar, R. H. Romero, and A. F. Maldonado, "Polarization propagators: A powerful theoretical tool for a deeper understanding of NMR spectroscopic parameters," Int. Rev. Phys. Chem. **29**, 1–64 (2010).

[11] C. Chang, M. Pelissier, and P. Durand, "Regular two–component Pauli–like effective Hamiltonians in Dirac theory," Phys. Scr. **34**, 394 (1986).

[12] E. v. Lenthe, E.-J. Baerends, and J. G. Snijders, "Relativistic regular two–component Hamiltonians," J. Chem. Phys. **99**, 4597–4610 (1993).

[13] E. van Lenthe, E.-J. Baerends, and J. G. Snijders, "Relativistic total energy using regular approximations," J. Chem. Phys. **101**, 9783–9792 (1994).

[14] J. Autschbach, "Relativistic effects on NMR parameters," in *Science and Technology of Atomic, Molecular, Condensed Matter & Biological Systems* (Elsevier, 2013), Vol. 3, pp. 69–117.

[15] J. Vícha, S. Komorovsky, M. Repisky, R. Marek, and M. Straka, "Relativistic spin–orbit heavy atom on the light atom NMR chemical shifts: General trends across the periodic table explained," J. Chem. Theory Comput. **14**, 3025–3039 (2018).

[16] P. Pyykkö, A. Görling, and N. Rösch, "A transparent interpretation of the relativistic contribution to the N.M.R. 'heavy atom chemical shift,'" Mol. Phys. **61**, 195–205 (1987).

[17] M. Kaupp, O. L. Malkina, V. G. Malkin, and P. Pyykkö, "How do spin–orbit-induced heavy–atom effects on NMR chemical shifts function? Validation of a simple analogy to spin–spin coupling by density functional theory (DFT) calculations on some iodo compounds," Chem. - Eur. J. **4**, 118–126 (1998).

[18] M. Douglas and N. M. Kroll, "Quantum electrodynamical corrections to the fine structure of helium," Ann. Phys. **82**, 89–155 (1974).

[19] B. A. Hess, "Applicability of the no–pair equation with free–particle projection operators to atomic and molecular structure calculations," Phys. Rev. A **32**, 756 (1985).

[20] B. A. Hess, "Relativistic electronic–structure calculations employing a two–component no–pair formalism with external–field projection operators," Phys. Rev. A **33**, 3742 (1986).

[21] G. Jansen and B. A. Hess, "Revision of the Douglas–Kroll transformation," Phys. Rev. A **39**, 6016 (1989).

[22] L. L. Foldy, "The electromagnetic properties of Dirac particles," Phys. Rev. **87**, 688–693 (1952).

[23] L. L. Foldy and S. A. Wouthuysen, "On the dirac theory of spin 1/2 particles and its non–relativistic limit," Phys. Rev. **78**, 29–36 (1950).

[24] J. I. Melo, M. C. Ruiz de Azúa, J. E. Peralta, and G. E. Scuseria, "Relativistic calculation of indirect NMR spin–spin couplings using the Douglas–Kroll–Hess approximation," J. Chem. Phys. **123**, 204112 (2005).

[25] S. Stopkowicz and J. Gauss, "Relativistic corrections to electrical first–order properties using direct perturbation theory," J. Chem. Phys. **129**, 164119 (2008).

[26] S. Stopkowicz and J. Gauss, "Direct perturbation theory in terms of energy derivatives: Fourth-order relativistic corrections at the Hartree–Fock level," J. Chem. Phys. **134**, 064114 (2011).

[27] S. Stopkowicz and J. Gauss, "Fourth–order relativistic corrections to electrical first–order properties using direct perturbation theory," J. Chem. Phys. **134**, 204106 (2011).

[28] L. Cheng, S. Stopkowicz, and J. Gauss, "Spin–free Dirac–Coulomb calculations augmented with a perturbative treatment of spin–orbit effects at the Hartree-Fock level," J. Chem. Phys. **139**, 214114 (2013).

[29] H. J. Aa. Jensen, "BSS/DKH infinite order the easy way!," paper presented at International Conference on Relativistic Effects in Heavy Element Chemistry and Physics (REHE 2005), Mülheim, Germany, 6–10 April 2005, available at https://doi.org/10.6084/m9.figshare.12046158.

[30] Q. Sun, W. Liu, Y. Xiao, and L. Cheng, "Exact two–component relativistic theory for nuclear magnetic resonance parameters," J. Chem. Phys. **131**, 081101 (2009).

[31] Q. Sun, Y. Xiao, and W. Liu, "Exact two–component relativistic theory for NMR parameters: General formulation and pilot application," J. Chem. Phys. **137**, 174105 (2012).

[32] K. G. Dyall, "Interfacing relativistic and nonrelativistic methods. I. normalized elimination of the small component in the modified Dirac equation," J. Chem. Phys. **106**, 9618–9626 (1997).

[33] K. G. Dyall, "Interfacing relativistic and nonrelativistic methods. II. Investigation of a low–order approximation," J. Chem. Phys. **109**, 4201–4208 (1998).

[34] K. G. Dyall, "Interfacing relativistic and nonrelativistic methods. IV. One– and two–electron scalar approximations," J. Chem. Phys. **115**, 9136–9143 (2001).

[35] V. M. Shabaev, I. I. Tupitsyn, V. A. Yerokhin, G. Plunien, and G. Soff, "Dual kinetic balance approach to basis–set expansions for the Dirac equation," Phys. Rev. Lett. **93**, 130405 (2004).

[36] R. E. Stanton and S. Havriliak, "Kinetic balance: A partial solution to the problem of variational safety in Dirac calculations," J. Chem. Phys. **81**, 1910–1918 (1984).

[37] H. Fukui, T. Baba, and H. Inomata, "Calculation of nuclear magnetic shieldings. X. Relativistic effects," J. Chem. Phys. **105**, 3175–3186 (1996).

[38] P. Manninen, P. Lantto, J. Vaara, and K. Ruud, "Perturbational *ab initio* calculations of relativistic contributions to nuclear magnetic resonance shielding tensors," J. Chem. Phys. **119**, 2623–2637 (2003).

[39] P. Manninen, K. Ruud, P. Lantto, and J. Vaara, "Leading–order relativistic effects on nuclear magnetic resonance shielding tensors," J. Chem. Phys. **122**, 114107 (2005).

[40] P. Manninen, K. Ruud, P. Lantto, and J. Vaara, "Erratum: 'leading–order relativistic effects on nuclear magnetic resonance shielding tensors' [J. Chem. Phys. 122, 114107 (2005)]," J. Chem. Phys. **124**, 149901 (2006).

[41] G. A. Aucar, J. I. Melo, I. A. Aucar, and A. F. Maldonado, "Foundations of the LRESC model for response properties and some applications," Int. J. Quantum Chem. **118**, e25487 (2018).

[42] J. I. Melo, M. C. Ruiz de Azúa, C. G. Giribet, G. A. Aucar, and R. H. Romero, "Relativistic effects on the nuclear magnetic shielding tensor," J. Chem. Phys. **118**, 471 (2003).

[43] J. I. Melo, M. C. Ruiz de Azua, C. G. Giribet, G. A. Aucar, and P. F. Provasi, "Relativistic effects on nuclear magnetic shielding constants in H*X* and CH_3X (X = Br, I) based on the linear response within the elimination of small component approach," J. Chem. Phys. **121**, 6798–6808 (2004).

[44] M. C. R. de Azúa, J. I. Melo, and C. G. Giribet, "Orbital contributions to relativistic corrections of the NMR nuclear magnetic shielding tensor originated in scalar field-dependent operators," Mol. Phys. **101**, 3103–3109 (2003).

[45] D. Zaccari, J. I. Melo, M. C. R. de Azúa, and C. G. Giribet, "Relativistic two-component geometric approximation of the electron–positron contribution to magnetic properties in terms of Breit–Pauli spinors," J. Chem. Phys. **130**, 084102 (2009).

[46]J. I. Melo, A. Maldonado, and G. A. Aucar, "Relativistic effects on the shielding of SnH_2XY and PbH_2XY (X, Y = F, Cl, Br and I) heavy atom–containing molecules," Theor. Chem. Acc. **129**, 483–494 (2011).
[47]A. F. Maldonado, G. A. Aucar, and J. I. Melo, "Core–dependent and ligand–dependent relativistic corrections to the nuclear magnetic shieldings in $MH_{4-n}Y_n$ (n = 0–4; M = Si, Ge, Sn, and Y = H, F, Cl, Br, I) model compounds," J. Mol. Model. **20**, 2417 (2014).
[48]I. A. Aucar, S. S. Gomez, C. G. Giribet, and M. C. Ruiz de Azúa, "Theoretical study of the relativistic molecular rotational g–tensor," J. Chem. Phys. **141**, 194103 (2014).
[49]I. A. Aucar, S. S. Gomez, C. G. Giribet, and G. A. Aucar, "Toward an absolute NMR shielding scale using the spin–rotation tensor within a relativistic framework," Phys. Chem. Chem. Phys. **18**, 23572–23586 (2016).
[50]J. I. Melo and A. F. Maldonado, "Relativistic corrections to the electric field gradient given by linear response elimination of the small component formalism," Int. J. Quantum Chem. **119**, e25935 (2019).
[51]J. J. Aucar, A. F. Maldonado, and J. I. Melo, "Relativistic corrections of the electric field gradient in dihalogen molecules *XY* (*X*, *Y* = F, Cl, Br, I, At) within the liaear response elimination of the small component formalism," Int. J. Quantum Chem. **121**, e26769 (2021).
[52]J. J. Aucar, A. F. Maldonado, and J. I. Melo, "High order relativistic corrections on the electric field gradient within the LRESC formalism," J. Chem. Phys. **157**, 244105 (2022).
[53]S. S. Gómez, J. I. Melo, R. H. Romero, G. A. Aucar, and M. R. de Azúa, "Relativistic corrections to the diamagnetic term of the nuclear magnetic shielding: Analysis of contributions from localized orbitals," J. Chem. Phys. **122**, 064103 (2005).
[54]A. D. Zapata−Escobar, A. F. Maldonado, and G. A. Aucar, "The LRESC–Loc model to analyze magnetic shieldings with localized molecular orbitals," J. Phys. Chem. A **126**, 9519–9534 (2022).
[55]A. D. Zapata-Escobar, A. F. Maldonado, J. L. Mendoza-Cortes, and G. A. Aucar, "NMR magnetic shielding in transition metal compounds containing cadmium, platinum, and mercury," Magnetochemistry **9**, 165 (2023).
[56]K. Aidas, C. Angeli, K. L. Bak, V. Bakken, R. Bast, L. Boman, O. Christiansen, R. Cimiraglia, S. Coriani, P. Dahle, E. K. Dalskov, U. Ekström, T. Enevoldsen, J. J. Eriksen, P. Ettenhuber, B. Fernández, L. Ferrighi, H. Fliegl, L. Frediani, K. Hald, A. Halkier, C. Hättig, H. Heiberg, T. Helgaker, A. C. Hennum, H. Hettema, E. Hjertenæs, S. Høst, I.-M. Høyvik, M. F. Iozzi, B. Jansík, H. J. A. Jensen, D. Jonsson, P. Jørgensen, J. Kauczor, S. Kirpekar, T. Kjærgaard, W. Klopper, S. Knecht, R. Kobayashi, H. Koch, J. Kongsted, A. Krapp, K. Kristensen, A. Ligabue, O. B. Lutnæs, J. I. Melo, K. V. Mikkelsen, R. H. Myhre, C. Neiss, C. B. Nielsen, P. Norman, J. Olsen, J. M. H. Olsen, A. Osted, M. J. Packer, F. Pawlowski, T. B. Pedersen, P. F. Provasi, S. Reine, Z. Rinkevicius, T. A. Ruden, K. Ruud, V. V. Rybkin, P. Sałek, C. C. M. Samson, A. S. de Merás, T. Saue, S. P. A. Sauer, B. Schimmelpfennig, K. Sneskov, A. H. Steindal, K. O. Sylvester-Hvid, P. R. Taylor, A. M. Teale, E. I. Tellgren, D. P. Tew, A. J. Thorvaldsen, L. Thøgersen, O. Vahtras, M. A. Watson, D. J. D. Wilson, M. Ziolkowski, and H. Ågren, "The dalton quantum chemistry program system," Wiley Interdiscip. Rev.: Comput. Mol. Sci. **4**, 269–284 (2014).
[57]G. A. Aucar and J. Oddershede, "Relativistic theory for indirect nuclear spin–spin couplings within the polarization propagator approach," Int. J. Quantum Chem. **47**, 425 (1993).
[58]L. Visscher, T. Saue, and J. Oddershede, "The 4–component random phase approximation method applied to the calculation of frequency–dependent dipole polarizabilities," Chem. Phys. Lett. **274**, 181–188 (1997).
[59]J. Oddershede, P. Jørgensen, and D. L. Yeager, "Polarization propagator methods in atomic and molecular calculations," Comput. Phys. Commun. **2**, 33–92 (1984).
[60]T. Saue and H. J. A. Jensen, "Linear response at the 4–component relativistic level: Application to the frequency–dependent dipole polarizabilities of the coinage metal dimers," J. Chem. Phys. **118**, 522–536 (2003).
[61]DIRAC, a relativistic *ab initio* electronic structure program, written by T. Saue, L. Visscher, H. J. A. Jensen, and R. Bast, with contributions from V. Bakken, K. G. Dyall, S. Dubillard, U. Ekström, E. Eliav, T. Enevoldsen, E. Faßhauer, T. Fleig, O. Fossgaard, A. S. P. Gomes, E. D. Hedegård, T. Helgaker, J. Henriksson, M. Iliaš, C. R. Jacob, S. Knecht, S. Komorovský, O. Kullie, J. K. Lærdahl, C. V. Larsen, Y. S. Lee, H. S. Nataraj, M. K. Nayak, P. Norman, G. Olejniczak, J. Olsen, J. M. H. Olsen, Y. C. Park, J. K. Pedersen, M. Pernpointner, R. di Remigio, K. Ruud, P. Sałek, B. Schimmelpfennig, A. Shee, J. Sikkema, A. J. Thorvaldsen, J. Thyssen, J. van Stralen, S. Villaume, O. Visser, T. Winther, and S. Yamamoto (2018). "DIRAC18 (v18.0)," Zenodo. https://doi.org/10.5281/zenodo.2253986, see also http://www.diracprogram.org.
[62]W. M. Haynes, *CRC Handbook of Chemistry and Physics* (CRC Press, 2014).
[63]N. B. Kagakkai, *Kagaku Benran*, 3rd ed. (Maruzen Company, 1984), Vol. 2, p. 649.
[64]H. Fujii and M. Kimura, "The molecular structure of tin tetrachloride as determined by gas–electron diffraction," Bull. Chem. Soc. Jpn. **43**, 1933–1939 (1970).
[65]M. Nagashima, H. Fujii, and M. Kimura, "Electron–diffraction investigation of the molecular structure of tetramethyltin," Bull. Chem. Soc. Jpn. **46**, 3708–3711 (1973).
[66]K. G. Dyall, "Relativistic quadruple–zeta and revised triple–zeta and double–zeta basis sets for the 4p, 5p, and 6p elements," Theor. Chem. Acc. **115**, 441–447 (2006).
[67]A. D. Becke, "A new mixing of Hartree–Fock and local density-functional theories," J. Chem. Phys. **98**, 1372–1377 (1993).
[68]M. Hanni, P. Lantto, M. Iliaš, H. J. A. Jensen, and J. Vaara, "Relativistic effects in the intermolecular interaction-induced nuclear magnetic resonance parameters of xenon dimer," J. Chem. Phys. **127**, 164313 (2007).
[69]J. I. Melo, A. F. Maldonado, and G. A. Aucar, "Performance of the lresc model on top of dft functionals for relativistic NMR shielding calculations," J. Chem. Inf. Model. **60**, 722–730 (2019).
[70]A. F. Maldonado and G. A. Aucar, "The UKB prescription and the heavy atom effects on the nuclear magnetic shielding of vicinal heavy atoms," Phys. Chem. Chem. Phys. **11**, 5615–5627 (2009).
[71]A. F. Maldonado and G. A. Aucar, "Relativistic and electron–correlation effects on the nuclear magnetic resonance shieldings of molecules containing tin and lead atoms," J. Phys. Chem. A **118**, 7863–7875 (2014).
[72]S. Hamaya and H. Fukui, "Dirac–Hartree–Fock perturbation calculation of magnetic shielding using the external field-dependent restricted magnetic balance condition," Bull. Chem. Soc. Jpn. **83**, 635–642 (2010).
[73]D. K. Hindermann and C. D. Cornwell, "Vibrational corrections to the nuclear–magnetic shielding and spin–rotation constants for hydrogen fluoride. Shielding scale for ^{19}F," J. Chem. Phys. **48**, 4148–4154 (1968).
[74]C. J. Jameson, A. K. Jameson, and S. M. Cohen, "Temperature and density dependence of ^{129}Xe chemical shift in rare gas mixtures," J. Chem. Phys. **62**, 4224–4226 (1975).
[75]A. F. Maldonado, J. I. Melo, and G. A. Aucar, "Theoretical analysis of NMR shieldings of group-11 metal halides on MX (M = Cu, Ag, Au; X = H, F, Cl, Br, I) molecular systems, and the appearance of quasi instabilities on AuF," Phys. Chem. Chem. Phys. **17**, 25516–25524 (2015).
[76]T. N. Mitchell, A. Amamria, B. Fabisch, H. G. Kuivila, T. J. Karol, and K. Swami, "Long–range tin–tin coupling constants: II. Two–bond coupling via carbon," J. Organomet. Chem. **259**, 157–164 (1983).
[77]J. J. Burke and P. C. Lauterbur, "Sn^1 nuclear magnetic resonance spectra^1," J. Am. Chem. Soc. **83**, 326–331 (1961).